Journal of Polymer Research (2020) 27: 54
https://doi.org/10.1007/s10965-020-2007-y

ORIGINAL PAPER

Synthesis and characterization of a novel Schiff base polyamide ligand and its copper(II) complex for comparative removal of Pb(II) ions from aqueous solutions

Marjan Aghaei[1] · Ali Hossein Kianfar[1] · Mohammad Dinari[1]

Received: 17 August 2019 / Accepted: 8 January 2020 / Published online: 7 February 2020

Abstract

A dicarboxylic acid Schiff base ligand was synthesized via condensation of 2-hydroxybenzaldehyde with 5-aminoisophthalic acid. The derived monomer was reacted with 4,4′-diaminodiphenyl ether and triphenyl phosphite (TPP) in tetrabutylammonium bromide (TBAB) molten ionic liquid as a green solvent to form an aromatic polyamide with a moderate yield (71%) and inherent viscosity (0.2 dL g^{-1}). The nanostructured copper(II)/polyamide complex was then prepared. The structure, optical properties, and morphology of the compositions were confirmed by FT-IR, $^{-1}$H-NMR, elemental analysis, UV-Vis, powder X-ray diffraction (XRD), thermogravimetric analysis (TGA) and field emission scanning electron microscopy (FE-SEM). The polyamide ligand and its nanostructured complex were comparatively applied in the elimination of Pb(II) ions from aqueous solutions.

Keywords Green chemistry · Lead · Metal ion adsorption · Nanostructure polyamide complex · Schiff base polymer

Introduction

The presence of heavy metals in aquatic systems has become a dangerous menace for environmental and general health [1]. Lead is one of the most important metals because of its high toxicity, even at extremely low concentrations [2] which results from mineral weathering and erosion, forest fires, volcanic activity [3], acid battery manufacturing, explosive manufacturing, mining, photographic materials, ceramic and glass industries [4, 5], fossil fuels combustion and smelting [6, 7].

Highlights
- The new PA containing Schiff base, was prepared in green solvent of TBAB.
- The synthesized PA was coordinated to Cu(II) ion to form metal polymer complex.
- The nanostructured PA ligand and its Cu(II) complex were comparatively applied to eliminate Pb(II) from water.
- The best adsorption was occurred at pH =6.

Electronic supplementary material The online version of this article (https://doi.org/10.1007/s10965-020-2007-y) contains supplementary material, which is available to authorized users.

✉ Ali Hossein Kianfar
akianfar@cc.iut.ac.ir

[1] Department of Chemistry, Isfahan University of Technology, Isfahan 84156/83111, Iran

Lead is mainly found in inorganic form particularly in the oxidation states of +II and + IV [8]. Since lead is nonbiodegradable [9] and can bioaccumulate in brain, bones, kidney, liver and muscles [10] and may cause many important health problems such as kidney disease, mental retardation, damage to the nervous system, cancer, anaemia [11], stillbirths, abortion, sterility and even neonatal deaths [10], it must be eliminated from water [9].

Many techniques such as chemical precipitation, ion exchange, membrane isolation, adsorption, etc. have been applied to eliminate Pb(II) from aquatic solutions. Most of these methods are not ideal due to their high cost and extensive processing [12]. Adsorption is the most preferred method for the removal of pollutants due to its simplicity and low cost [13]. Many adsorbents such as functionalized polymeric materials have been utilized to eliminate lead [14–18] owing to the capability of active sites on polar polymers for adsorption of metal ions [19–21].

Aromatic polyamides (PAs) are among important functionalized polymeric compounds, because they have been used in numerous applications considering their thermal, mechanical and chemical properties [22–24]. The existence of azomethine groups in the polymer structure not only elevates the thermal durability, but also enhances its protonation and complexation capability [25–27].

In the current research, we report a nanostructured aromatic PA comprising azomethine in the side chain, which is prepared via polycondensation of (*E*)-5-(2-hydroxybenzylideneamino)isophthalic acid and 4,4′-diaminodiphenyl ether in tetrabutylammonium bromide (TBAB). This novel PA is then attached to Cu(II) to form a metal polymer complex. FE-SEM analysis indicates porous buildings of the synthesized polymers. Subsequently, the removal of Pb(II) ions from aqueous solutions by these compounds (PA ligand and its complex) has been compared. To achieve this target, the impacts of different factors such as pH, contact time, initial concentration of Pb(II) and temperature have been investigated.

Experimental

Materials and methods

All the chemicals and solvents used in current research were purchased from Merck and Aldrich Chemical Co. A Perkin Elmer JASCO V-570 double beam spectrophotometer was used to perform UV-Vis spectroscopy in the range of 200–800 nm. FT-IR spectra were recorded using a JASCO-680 spectrophotometer in the 400–4000 cm^{-1} range. A model XRD Philips X'PERT MPD was used to perform X-ray diffraction analysis (XRD) on the slope 2θ, 10 to 100 degrees. A Bruker AVANCE 500 MHz spectrometer was used to record the ^{1}H-NMR spectra in DMSO solvent. Pore sizes were determined by Field Emission Scanning Electron Microscopy (FE-SEM) using a model MIRA3_ LMU (TESCAN). A STA503 TA instrument was used to record TGA curves at a heating rate of 10 °C min^{1-} from room temperature to 800 °C in the milieu of argon. Carbon, hydrogen and nitrogen values of the combinations were assigned via a Perkin Elmer Seris elemental analyzer. Inherent viscosity was evaluated by a modulus mode per a Cannon-Fenske normal viscometer at the concentration of 0.5 dL g^{-1} at room temperature. Using a flame atomic adsorption spectrometer (FAAS, PerkinElmer), the amount of Pb(II) ions was determined.

Synthesis of (E)-5-(2-hydroxybenzylideneamino) isophthalic acid Schiff base ligand (L)

5-aminoisophthalic acid [1.812 g, 10 mmol] was reacted with salicylaldehyde [1.22 g, 10 mmol] in methanol at reflux for 2 h to yield (*E*)-5-(2-hydroxybenzylideneamino)isophthalic acid Schiff base ligand [28]. The final product (**L**) (^{1}H-NMR in Fig. S1), which was an orange precipitate [29], was filtered and washed with methanol.

Synthesis of aromatic PA ligand including azomethine in the side chain (poly-L)

The mixture of **L** ligand, 4,4′-diaminodiphenyl ether and TBAB was placed in a flask. Having heated the mixture at 150 °C for half of hour, 1.7 mL of triphenylphosphite (TPP), were added. The reaction was carried out at 130 °C for 16 h. After cooling, 10 mL of methanol were added to the mixture, which was then stirred at 60 °C for half of hour. The obtained solid was filtered, washed with methanol and boiling water and dried. Finally, the product was purified via dissolution in DMF and recrystallization via adding methanol. The yield 71% and inherent viscosity 0.2 dL g^{-1} were attained for poly-L (^{1}H-NMR in Fig. S2) [29]. The structure of poly-L polymeric ligand is displayed in Scheme 1.

Synthesis of the PA Cu(II) Schiff base complex (complex poly-L/Cu(II))

Copper(II) acetate (0.15 mmol, 0.03 g) was transferred to a methanol (20 mL) solution of **poly-L** ligand (0.15 mmol, 0.07 g). The gained mixture was stirred and refluxed for 2 h at 50 °C. The green residue was separated via gravity filtration, washed with methanol, and dried at room temperature.

Complex poly-L/Cu(II) Elemental Analysis. Calculated. For $(C_{29}H_{21}N_3O_6Cu$ (571 g/mol)$_n$: C 60.95%; H 3.68%; N 7.36%. Found: C 60.52%; H 3.65%; N 7.34%. UV-Vis (DMF): λ_{max} (nm): 259, 298, 336, 471, 515, 690 and 789.

Adsorption experiments

The comparative removal of lead by poly-L ligand and poly-L/Cu(II) complex was performed according to the batch equilibrium method in aqueous solutions, the target pH being kept constant using dilute CH_3COONa/CH_3COOH solutions.

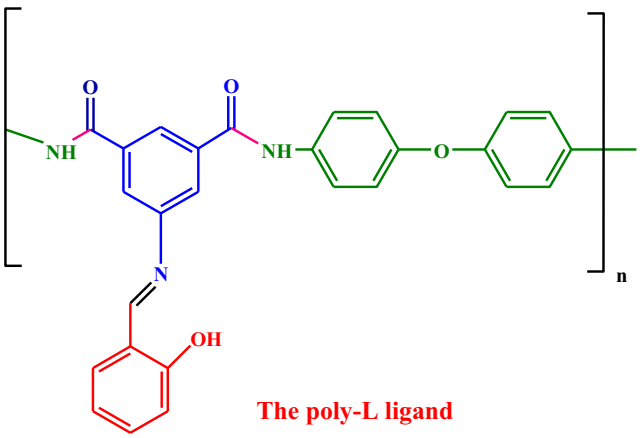

Scheme 1 The structure of poly-L polymeric ligand

Separately, 2 mg of poly-L and poly-L/Cu(II) complex adsorbents were added to 4 mL of Pb(II) [$Pb(OAc)_2$] solution. The mixture obtained was stirred for 30 min at 200 rpm to facilitate the adsorption of lead on the PA ligand and its complex. Atomic adsorption spectrometry (FAAS, Perkin Elmer) was used to determine the ion content in the solution. The studies were performed under these conditions: pH: 3–8, metal ion concentration (15–35 and 15–100 mg L^{-1} for the poly-L ligand and poly-L/Cu(II) complex, respectively), contact time: 5–50 min, and temperature: 30–60 °C. The removal efficiency (*R%*) of the metal was calculated by Eq. (1).

$$R\% = [(C_o - C_e)/C_o] \times 100 \quad (1)$$

where C_o and C_e (mg L^{-1}) are the initial and equilibrium concentrations of lead in the solution, respectively. The equilibrium adsorption ability was found using Eq. (2).

$$q_e = (C_o - C_e)V/W \quad (2)$$

in which *V* is the total solution volume (L) and *W* is the adsorbent mass (g).

Results and discussion

In current work, polymeric ligand was synthesized by the polymerization of 5-aminoisophthalic acid containing diacid with 4,4′-diaminodiphenyl ether in the existence of TBAB ionic liquid. Scheme 1 shows the plot of the reaction. Poly-L ligand was capable of forming a complex via imine and phenolic OH. In the next step, poly-L/Cu(II) complex was prepared in methanol. The structure of the products was investigated by elemental analysis and FT-IR. One salycilaldimine from Poly-L ligand and acetate ion were coordinated to the copper(II) ion, according to the results of the elemental analysis of the complex. Scheme 2 shows a proposed structure containing these compounds based on previous studies [30–32].

FT-IR spectra

Figure 1 shows the FT-IR spectra of **L** ligand, poly-L aromatic ligand, and poly-L/Cu(II) complex. A broad peak is observed in the spectrum of **L** ligand (Fig. 1a) in the range of 3100–3400 cm^{-1}, which corresponds to the vibrational frequency of carboxylic acid and phenolic OH groups. The sharp band at 1725 cm^{-1} is associated with carboxylic acid groups. The azomethine (C=N) group appears at 1629 cm^{-1}. As poly-L ligand forms (Fig. 1b), the wide peak due to the carboxylic acid disappears and a novel peak is observed at about 3200–3500 cm^{-1}, corresponding to the overlap of the phenolic OH and amidic NH groups in the poly-L structure. The intense band at 1659 cm^{-1} is

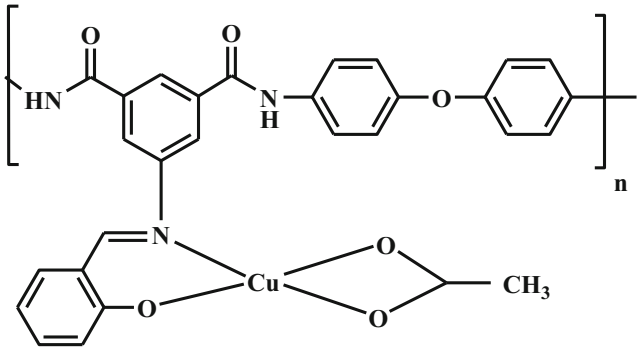

Scheme 2 The Proposed structure of the poly-L/Cu(II) complex

associated with the amidic carbonyl group. The presence of carbonyl bands at lower frequencies, in comparison with **L** monomer ligand, confirms the formation of amide. Furthermore, the frequencies of poly-L ligand shift to lower values upon copper ion coordination to the ligand. This is likely due to the resonance in the amide, which weakens the C=O bond [33, 34]. The azomethine group of poly-L ligand can be observed at 1599 cm^{-1}, which moves to a lower frequency in comparison with **L** monomer ligand. The equal bands at 1498 and at around 1230 cm^{-1} for poly-L ligand and poly-L/Cu(II) complex are attributed to the vibrations of C=C and C—O groups, respectively. The broad band in the 3200–3500 cm^{-1} range in the spectrum of the poly-L/Cu(II) complex (Fig. 1c) is due to the OH groups of methanol molecules in the surrounding of the complex.

Electronic spectra

The UV-Vis spectra of **L**, poly-L ligands and poly-L/Cu(II) complex were recorded at ambient temperature in DMF solvent in the range of 200–800 nm (Fig. 2). An absorption band and a shoulder are observed at 268 and 296 nm, respectively, in the electronic spectrum of **L** ligand (Fig. 2a), which are attributed to the intraligand $\pi \rightarrow \pi^*$ transitions of the aromatic rings. In addition, the peak at 344 nm corresponds to the $\pi \rightarrow \pi^*$ transition of the azomethine group [35]. The strong peak at 276 nm in the UV-Vis spectrum of the poly-L ligand (Fig. 2b) could be due to intraligand transition ($\pi \rightarrow \pi^*$) [33]. This transition has shifted to the higher energy area compared with **L** ligand. The bands observed in 259–336 nm range in the spectrum of poly-L/Cu(II) complex (Fig. 2c) are attributed to intraligand transitions ($\pi \rightarrow \pi^*$ and $n \rightarrow \pi^*$) and CT transitions between the metal and the ligand. However, these transitions overlap together and it is not possible to clearly assign the peaks [33]. On the other hand, poly-L/Cu(II) complex was not completely soluble in DMF and thus the determination

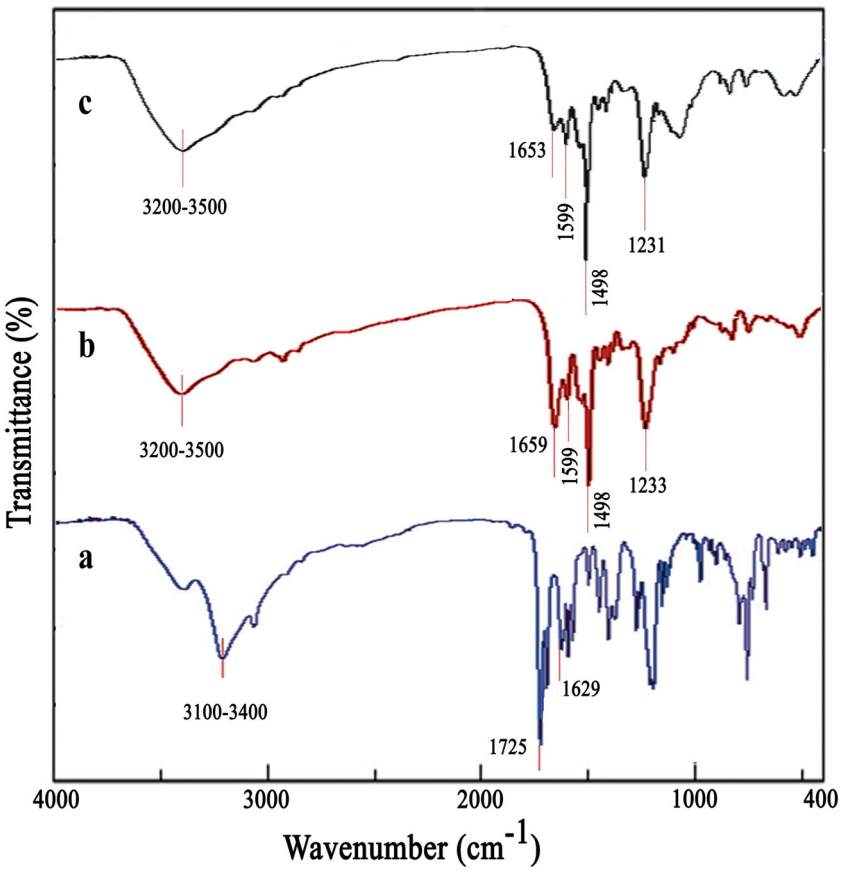

Fig. 1 IR-Spectra of (a) the L monomeric ligand, (b) the poly-L ligand, and (c) the poly-L/Cu(II) complex

of absorption coefficient (ε) was not possible. In addition, considering the low intensity, the bands in the 471–789 nm range are due to the d-d transitions of the copper(II) ion in the complex.

Surface morphology studies

The surface morphology of the novel PA ligand and its complex are displayed in Fig. 3. As clearly observed in Fig. 3a, c

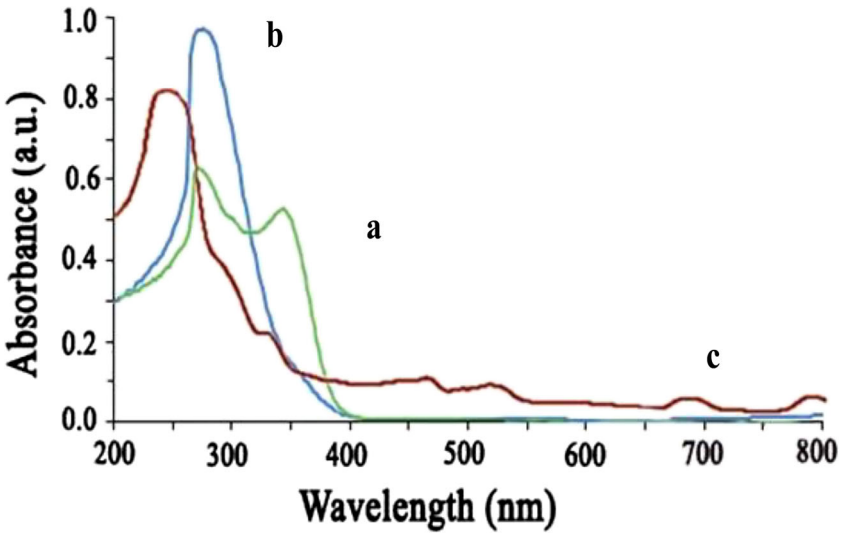

Fig. 2 The UV-Vis spectra of (a) the L monomeric ligand, (b) the poly-L ligand, and (c) the poly-L/Cu(II) complex

are the FE-SEM images of the poly-L ligand and poly-L/Cu(II) complex before adsorption of lead ions, there are porous surfaces appropriate for adsorption. Based on the FE-SEM images following the adsorption of lead ions (Fig. 3b, d), the surface morphology of the poly-L ligand and poly-L/Cu(II) complex have changed (spherical surfaces), which is probably due to the presence of lead ions adsorbed on the PA surfaces. This observation proposes that the adsorbents owe suitable morphology for lead adsorption and the lead ions get adsorbed on the functional groups in the wall of PAs [36].

Nitrogen adsorption-desorption analysis

According to IUPAC notation, microporous, mesoporous and macroporous materials possess pore diameters in the range of 2 nm > D, 2 nm < D < 50 nm, and D > 50 nm, respectively. The resulting nitrogen adsorption-desorption isotherms of both poly-L ligand and poly-L/Cu(II) complex can be categorized as type-IV isotherms by the IUPAC classification with narrow hysteresis, indicating the presence of mesopores in both poly-L ligand and poly-L/Cu(II) complex structures (Fig. 4a, b). The peaks centered at 1.72 and 7.98 nm for poly-L ligand and poly-L/Cu(II) complex, respectively, (Fig. 4c, d) are shown by the pore size distribution data from the desorption branches of nitrogen isotherms, according to the Barret-Joyner-Halenda (BJH) method. Table 1 shows the textural properties; that is, surface area, total pore volume, and pore size diameter (BET/BJH) of both samples. The values of the surface area, total pore volume and pore size distribution have increased following complexation, as observed.

X-ray diffraction analysis

The XRD patterns of poly-L ligand and poly-L/Cu(II) complex are shown in Fig. 5. Based on the patterns, these compounds display the presence of a small amount of crystalline phases compared with an amorphous one because polyamides could form hydrogen bonds and become ordered [37]. Three reflections, consisting of one strong peak and two weak ones, are observed at 2θ values of 10^{o}-100^{o} in the high angle diffraction pattern of the ligand. Nevertheless, the intensity of these wide diffraction peaks was observed to increase in the complex without varying the peak positions in comparison with the poly-L ligand. This perseverance of peak places

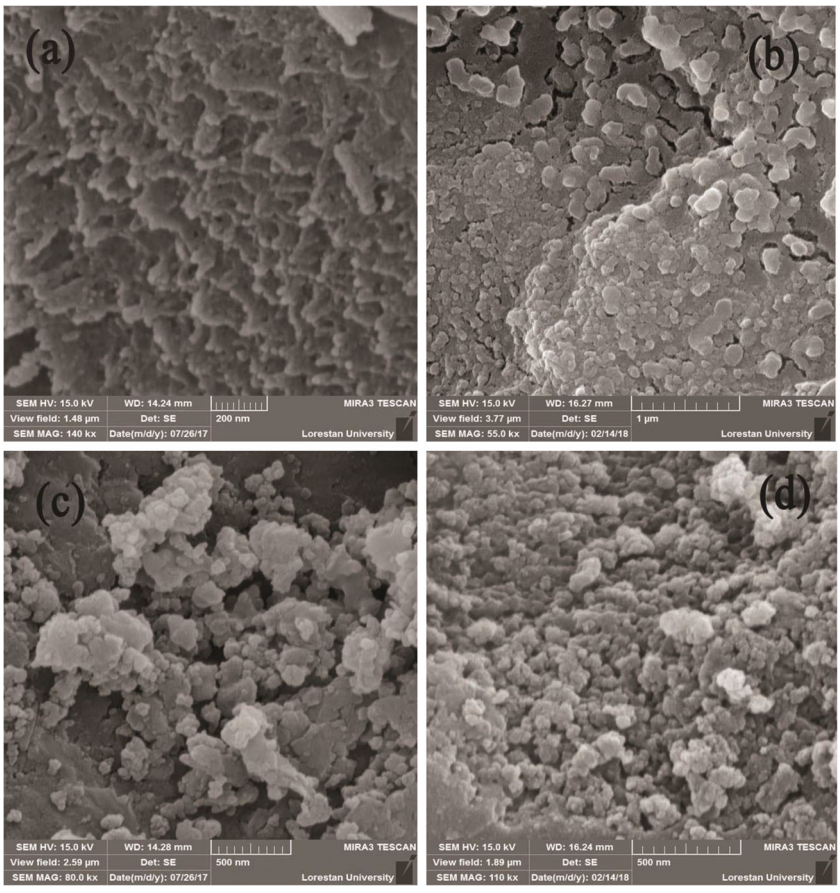

Fig. 3 FE-SEM images of PAs and metal adsorbed PAs. **a** poly-L, **b** Pb(II) adsorbed poly-L, **c** the poly-L/Cu(II) complex, and **d** Pb(II) adsorbed poly-L/Cu(II) complex

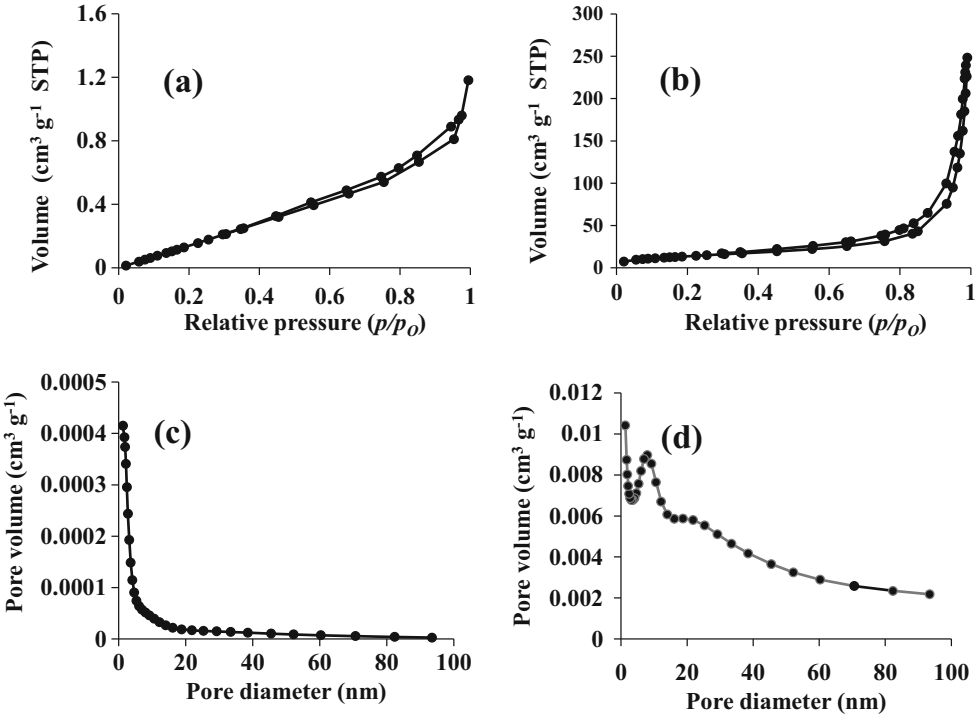

Fig. 4 Nitrogen adsorption-desorption isotherms of **a** the poly-L ligand and **b** the poly-L/Cu(II) complex at 77 K, corresponding BJH pore size distributions obtained from the adsorption branch of the isotherm for **c** the poly-L ligand and **d** the poly-L/Cu(II) complex

indicates the structural stability of the poly-L after coordination to metal ions.

Thermogravimetric analysis

The thermal behavior of the PAs was studied by TGA technique. The TGA measurements of the poly-L ligand and poly-L/Cu(II) complex were done in the range of 25–800 °C at a rate of 10 °C min^{1-} under argon atmosphere. Figure 6 shows the resulting obtained. A two or four step weight loss is shown by the curves of polymers. The initial weight loss (1–6%, *w/w*) was observed in the 50–100 °C temperature range, corresponding to the solvent loss. A mass loss about 20% is shown by the poly-L ligand in the temperature range of 300–400 °C. Nevertheless, a slight weight decrease was observed in the corresponding temperature range upon coordination to the Cu(II) ion, which indicates the enhanced thermal stability of the complex. Again, with increase in the temperature of up to 800 °C, the poly-L retained 33.5% of its initial weight while poly-L/Cu(II) complex retained 50% of its initial weight, which proved that the thermal stability of PA ligand is enriched by its coordination to the Cu(II) ion.

Use of the nanostructured PA ligand and its complex for Pb(II) adsorption

The effect of solution pH

The pH effect on the adsorption ability of Pb(II) by poly-L ligand and poly-L/Cu(II) complex is shown in Fig. 7. For both poly-L and poly-L/Cu(II) complex adsorbents, the pH values varied from 3 to 8 (in the initial concentration of 20 ppm for Pb(II) with 0.002 g of adsorbents at the room temperature and contact time of 30 min). The adsorption capacities of the PAs was raised by increasing pH from 3 to 6 and then reduced. At acidic pH values, protonation of the adsorbing sites (azomethine and amide) occurred in the PAs and the metal ion removal was minimal, seemingly owing to the greater

Table 1 Pore volume (*V*), specific surface area (*S*) and pore size (*D*) of the poly-L ligand and the poly-L/Cu(II) complex according to the BET and BJH models

	BET			BJH		
Sample	V_{BET} (cm^3/g)	S_{BET} (m^2/g)	D_{BET} (nm)	V_{BJH} (cm^3/g)	S_{BJH} (m^2/g)	D_{BJH} (nm)
Poly-L ligand	0.1043	0.45395	15.301	0.0019969	1.071	1.72
Poly-L/Cu(II) complex	11.59	50.444	30.143	0.3862	58.964	7.98

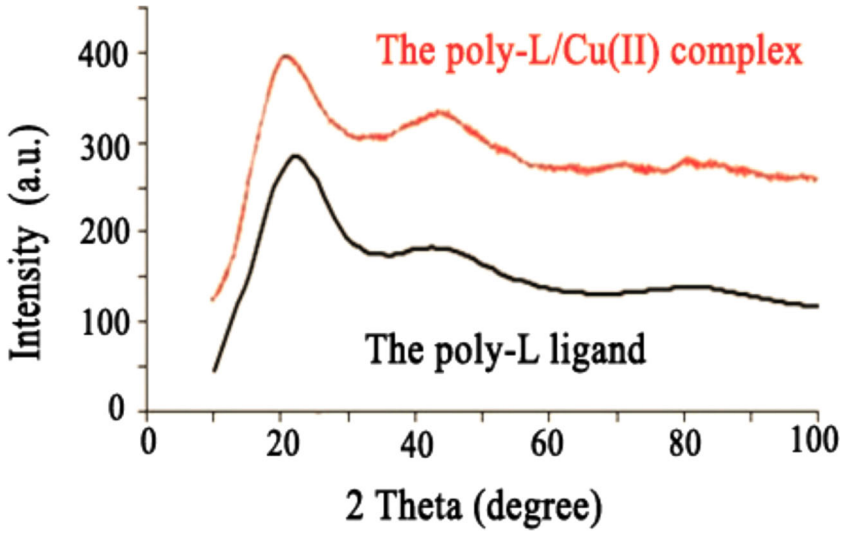

Fig. 5 X-ray diffraction patterns of the poly-L ligand and the poly-L/Cu(II) complex

competition of H^+ with metal ions for the binding sites and complex construction. As the pH of solution enhanced, the functional groups of the adsorbents were deprotonated. Therefore, the Pb(II) ions could simply bind to the adsorption sites. With increase of pH from 6 to 8, the OH^- ion concentration was increased and the metal ions seemed as $M(OH)_2$. For further studies, an optimal pH value of 6 was selected for both the adsorbents. As a result, the adsorption capacity of poly-L ligand was higher than that of poly-L/Cu(II) complex for the removal of lead from water because the former had more active sites in comparison with its complex.

The effect of contact time on the adsorption of Pb(II)

One of the important factors in the adsorption of metal ions is the contact time. This factor was probed at various times in the range of from 5 to 50 min and at the optimum pH of 6 to study the effect of contact time upon the adsorption rate by poly-L ligand and poly-L/Cu(II) complex. Initial concentrations were kept at 35 mg L^{-1} and 100 mg L^{-1} of Pb(II) for poly-L and poly-L/Cu(II) complex, respectively. The removal percentage of the metal ions was plotted (Fig. 8). There was a rapid adsorption of lead up to 30 min contact time. Therefore, over 96% of Pb(II) was adsorbed by both poly-L and poly-L/Cu(II) complex adsorbents. This fast adsorption phenomenon was due to the presence of large number of active sites available for lead adsorption. The removal percentage of the metal ions decreased beyond the contact time of 30 min. Hence, an optimum contact time of 30 min was chosen for further experiments.

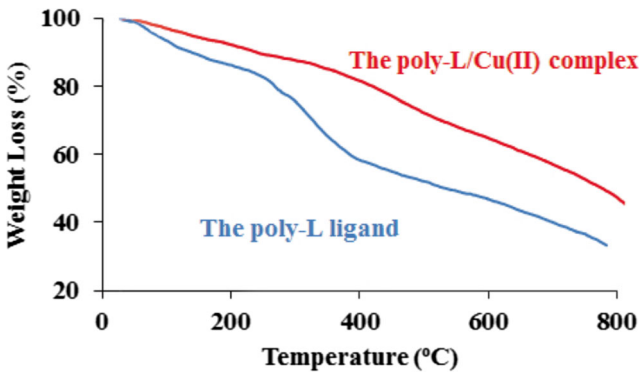

Fig. 6 TGA thermograms of the poly-L ligand and the poly-L/Cu(II) complex

Two kinetic models were used to investigate the adsorption kinetics of the metal ions [38, 39]. Equation (3) shows the pseudo-first-order model, in which k_1 is the rate constant (min^{-1}), and q and q_e are the adsorption capacity at time t and equilibrium (mg g^{-1}), respectively.

$$Log\ (q_e - q) = log\ q_e - (k_1 t/2.303) \quad (3)$$

The pseudo-second-order model is observed as follows (Eq. (4)).

$$t/q = 1/k_2 q_e^{\ 2} + t/q_e \quad (4)$$

where k_2, is the rate constant of the pseudo-second-order (g (mg min) $^{-1}$).

The kinetic model with a higher correlation coefficient, R^2, was selected as the best model.

The pseudo-second-order model [40–42] was found to possess the highest compatibility with the experimental data compared with the pseudo-first-order model for studying the adsorption mechanism of Pb(II) ions by poly-L ligand and poly-L/Cu(II) complex (Table 2).

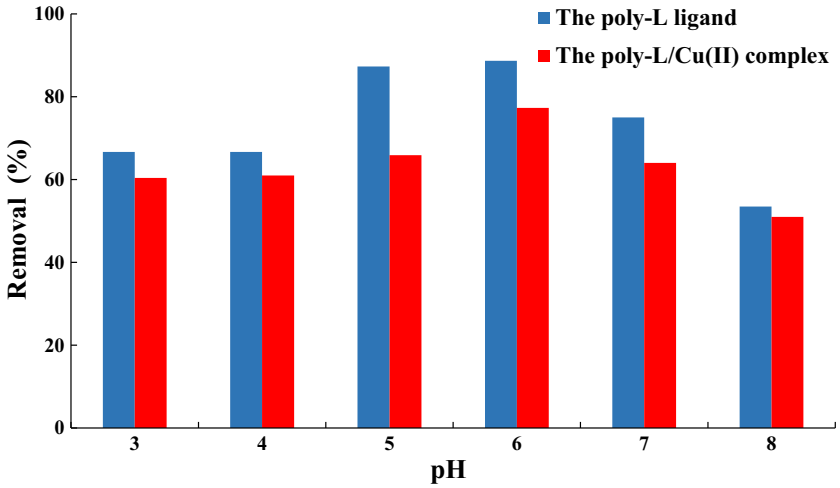

Fig. 7 The effect of pH on adsorption of Pb(II) by the poly-L ligand (red) and the poly-L/Cu(II) complex (orange)

The effect of temperature

An important factor for the adsorption of lead ions onto poly-L and poly-L/Cu(II) complex adsorbents is the temperature of the solution. Increased or decreased temperature can vary the equilibrium capacity of the adsorbents within the attraction. The results of the experiments performed at the temperature range of 30–60 °C are shown in Fig. 9. Pb(II) adsorption onto poly-L nanoadsorbent was studied by increasing the temperature from 30 to 60 °C. It was found that the equilibrium capacity enhanced with increase in temperature. Therefore, the adsorption was considered an endothermic process (Fig. 9a). Increased temperature provides a number of active sites with lower resistance for diffusion of metal ions toward the active sites [43]. The adsorption of Pb(II) on poly-L/Cu(II) complex was studied in the temperature range of 30–60 °C (Fig. 9b). The adsorption capacity decreased from 30 to 40 °C, but it increased up to 60 °C. Thus, the adsorption was endothermic.

The effect of Pb(II) concentration and adsorption isotherm

The equilibrium adsorption of Pb(II) onto poly-L ligand and poly-L/Cu(II) complex adsorbents was investigated by Langmuir and Freundlich models. Therefore, some experiments were carried out using different initial Pb(II) concentrations (15 to 35 ppm for poly-L and 15 to 100 ppm for poly-L/Cu(II) complex) with 0.002 g of the adsorbents at a pH = 6 and contact time of 30 min.

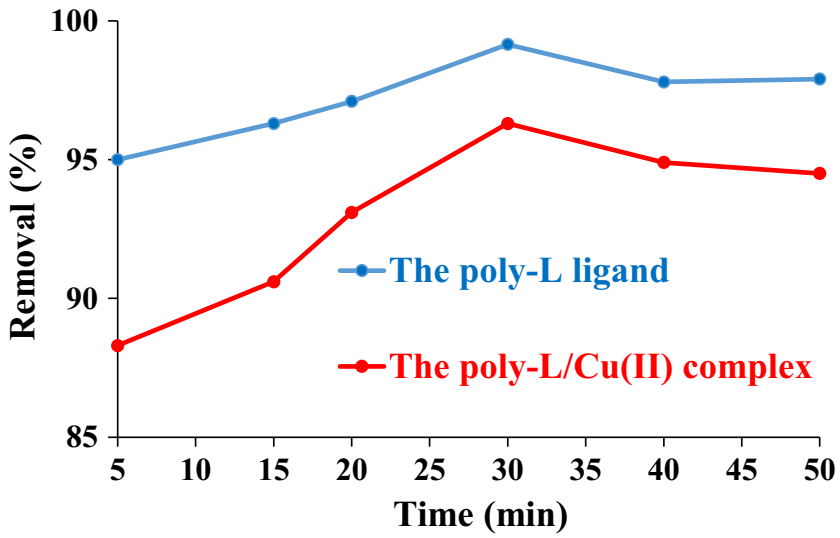

Fig. 8 The effect of contact time on adsorption of Pb(II) via the poly-L ligand and the poly-L/Cu(II) complex (pH = 6)

Table 2 Comparison of the kinetic parameters for the **poly-L** and the **poly-L/Cu(II) complex** in Pb(II) adsorption

Sorbent	$q_e(exp)$ (mg/g)	Pseudo-first order			Pseudo-second order		
		$q_{e,cal}$ (mg/g)	$k_1(min^{-1})$	R^2	$q_{e,cal}$ (mg/g)	k_2 (mg (g min)$^{-1}$)×10^{-3}	R^2
Poly-L	69.4	2.887	0.0258	0.9327	68.49	59.2	0.9998
Poly-L/Cu(II) complex	192.6	17.76	0.0380	0.8586	188.68	11.7	0.9991

Adsorption isotherms show adsorption interaction with the adsorbents and are thus important in the optimization of the adsorbents. Therefore, there are no interactions among the adsorbed molecules in Langmuir model and adsorption takes place on homogeneous surfaces.

The Langmuir isotherm equation can be expressed as [44].

$$C_e/q_e = 1/K_L.q_m + C_e/q_m \quad (5)$$

in which C_e (mg L^{-1}) is the equilibrium concentration, q_e (mg g^{-1}) is the adsorption capacity at equilibrium, q_m (mg g^{-1}) is the maximum adsorption capacity of the adsorbents, and the Langmuir constant, K_L, is related to the adsorption energy or net enthalpy (L mg^{-1}) (Fig. 10a).

Freundlich model can be used to describe the multi-layer adsorption of an adsorbate onto the heterogeneous surface of the adsorbent. The Freundlich model is expressed as:

$$ln\, q_e = ln\, K_F + ln\, C_e/n \quad (6)$$

The constant K_F expresses the adsorption capacity (L g^{-1}) and the experimental factor n is related to adsorption intensity (Fig. 10b). Table 3 displays the parameters and constants of both models for the poly-L ligand and poly-L/Cu(II) complex adsorbents.

The R^2 values obtained from Langmuir models for Pb(II) by poly-L and poly-L/Cu(II) complex were 0.9999 and 0.9997, respectively. The corresponding

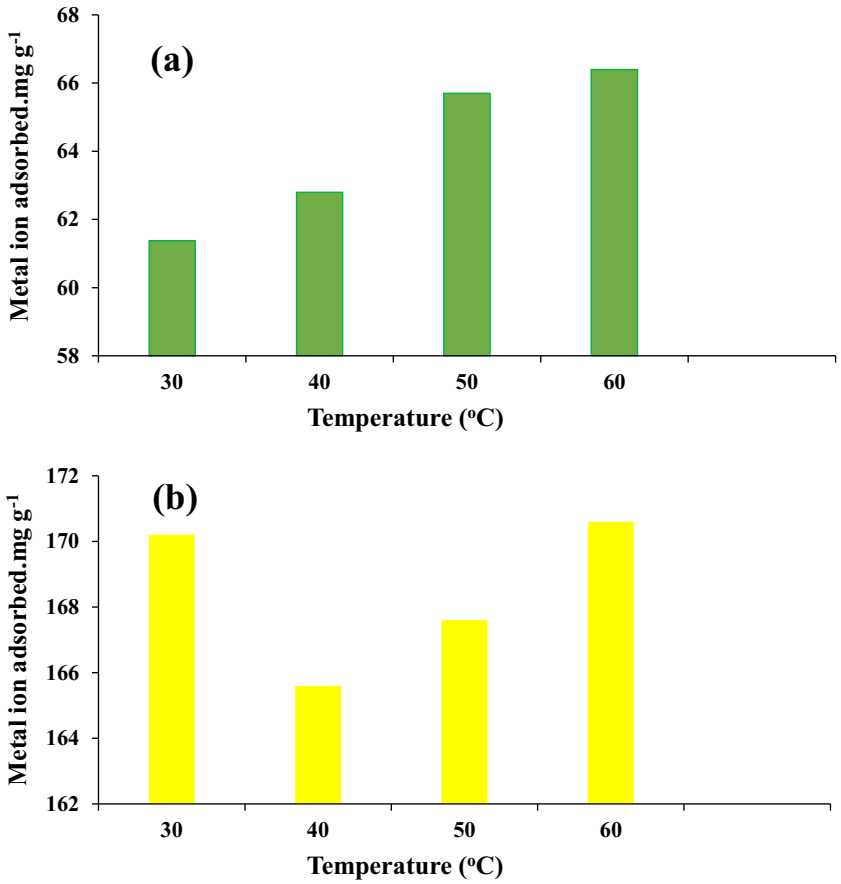

Fig. 9 The effect of temperature on adsorption of Pb(II) by **a** the poly-L ligand and **b** the poly-L/Cu(II) complex for 30 min at pH = 6

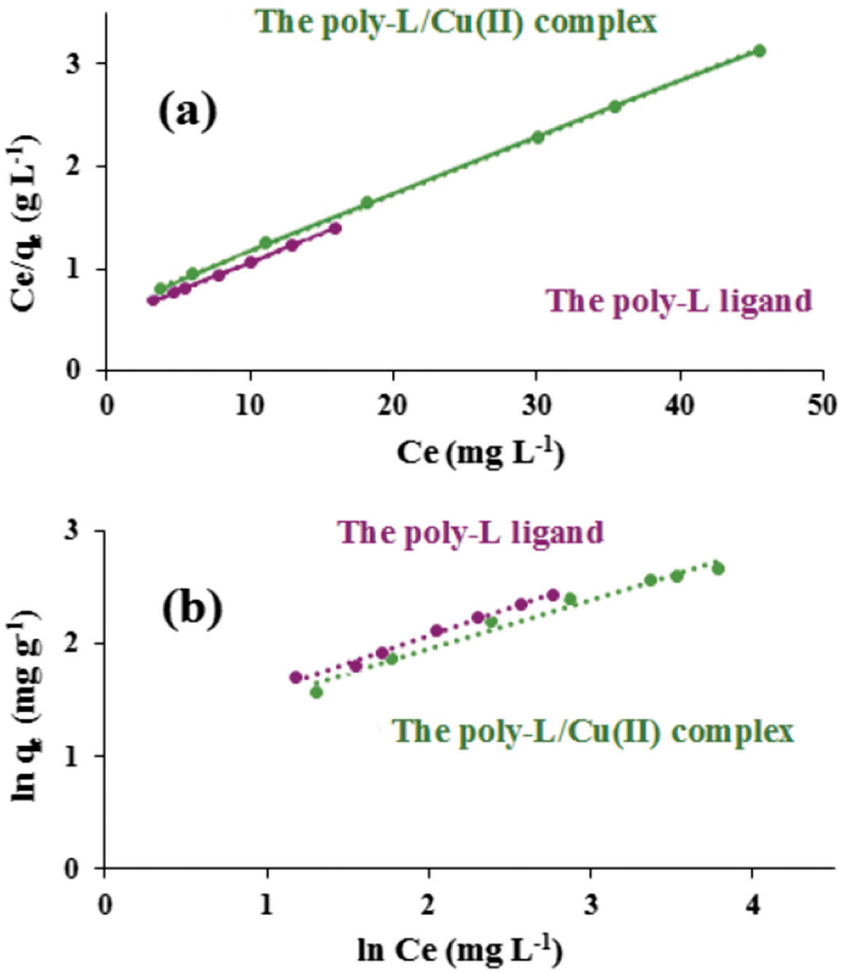

Fig. 10 The effect of concentration **a** Langmuir adsorption isotherm and **b** Freundlich adsorption isotherm for the adsorption of Pb(II) on the poly-L ligand and the poly-L/Cu(II) complex

values found using the Freundlich model were 0.9907 and 0.9786, respectively, which are somewhat smaller, proposing that the Langmuir isotherm is the best model to describe the adsorption of Pb(II) onto the two adsorbents. The values of n in Freundlich model for the poly-L ligand and poly-L/Cu(II) complex were 2.0547 and 2.3332, respectively. The values of n greater than 1 in the adsorption process are favorable [45] and suggest a physical adsorption. The maximum adsorption capacity (q_m) values for Pb(II) ions with the poly-L and poly-L/Cu(II) complex adsorbents were 17.95 and 17.64 mg g^{-1}, respectively.

To study the structural properties of the nanostructured polymeric ligand and its complex after the adsorption of lead ions, the FE-SEM and EDX images of the compounds were recorded. The EDX of samples (Fig. 11) showed the presence of lead ions. Thus, the adsorption happened, but no ions were exchanged.

The proposed mechanism of the adsorption of Pb(II) ions by the poly-L ligand and the poly-L/Cu(II) complex is displayed in Fig. S3.

Table 3 Adsorption capacities and comparison of Langmuir and Freundlich isotherm models for adsorption of Pb(II) onto poly-L and poly-L/Cu(II) complex

	Langmuir isotherm model			Freundlich isotherm model		
Adsorbents	q_m (mg/g)	K_L (L/mg)	R^2	K_F (mg/g)	n	R^2
Poly-L	17.95	0.1101	0.9999	3.0138	2.0547	0.9907
Poly-L/Cu(II)	17.64	0.1006	0.9997	3.0505	2.33320.9786	

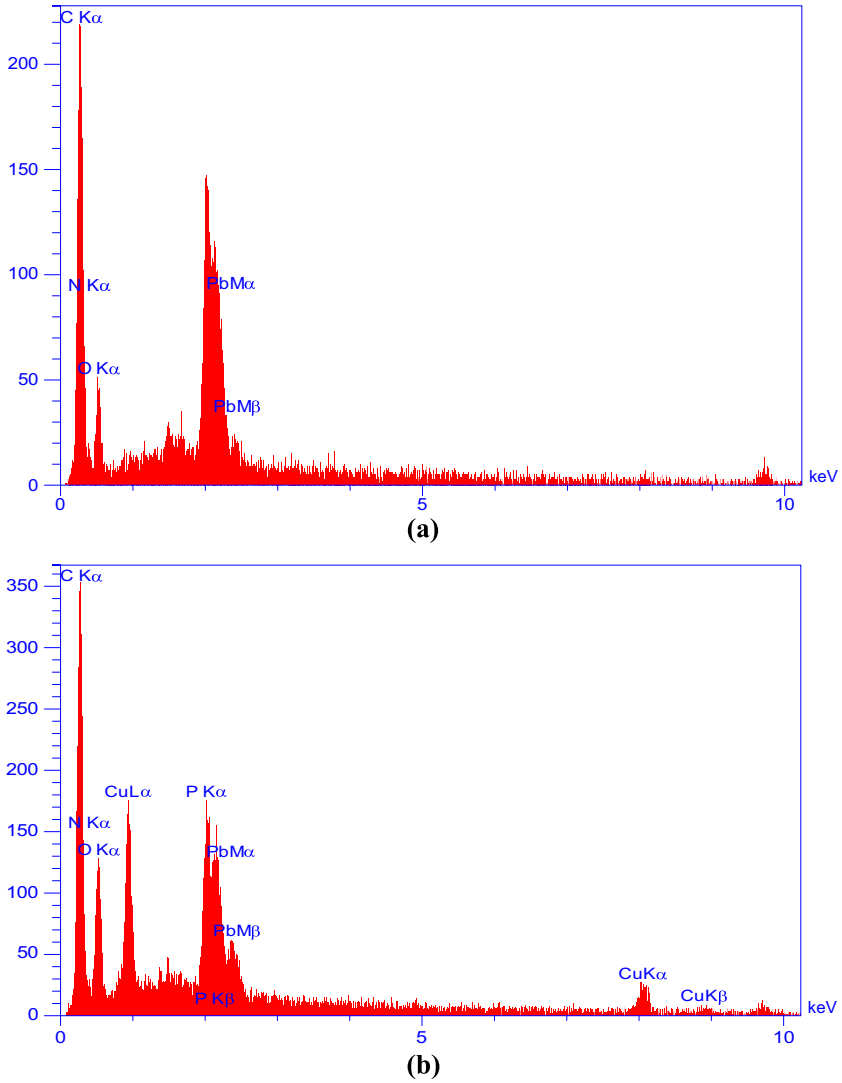

Fig. 11 SEM/EDX spectra of **a** the Pb(II) loaded poly-L and **b** the Pb(II) loaded poly-L/Cu(II) complex

Conclusion

The novel PA ligand containing a Schiff base in the side chain was produced via polymerization of (*E*)-5-(2-hydroxybenzylideneamino)isophthalic acid and 4,4′-diaminodiphenyl ether in tetrabutylammonium bromide (TBAB). This PA ligand was then coordinated to the Cu(II) ion to form the metal-polymer complex. TGA, XRD, FT-IR and UV-Vis methods were used to characterize the samples. FE-SEM analysis displayed that PA ligand and its complex had nano sized holes. The synthesized nanostructured PA ligand and complex were used to remove Pb(II) ions from water. The adsorption was significantly dependent on contact time, temperature, initial concentration of metals, and pH. The best adsorption occurred at pH = 6. The rate of Pb(II) attractions on the adsorbents followed the pseudo-second-order model. The equilibrium isotherm data for Pb(II) ions adsorption were fitted to the Langmuir model for PA ligand and its complex. Furthermore, the maximum adsorption capacity (q_m) of poly-L was more than that of poly-L/Cu(II) complex due to more active sites of the former.

Acknowledgements The authors appreciate Isfahan University of Technology (IUT) for partial financial support of this work.

Compliance with ethical standards

Conflict of interest The authors expressed that they own no conflicts of interest in current research.

References

1. Feng Z, Zhu S, Martins de Godoi DR, Samia AC, Scherson D (2012) Adsorption of Cd2+ on carboxyl-terminated

superparamagnetic iron oxide nanoparticles. Anal Chem 84:3764–3770
2. Ahmedna M, Marshall WE, Husseiny AA, Rao RM, Goktepe I (2004) The use of nutshell carbons in drinking water filters for removal of trace metals. Water Res 38:1062–1068
3. Krause-Nehring J, Brey T, Thorrold SR (2012) Centennial records of lead contamination in northern Atlantic bivalves (Arctica islandica). Mar Poll Bull 64:233–240
4. Yetilmezsoy K, Demirel S, Vanderbei RJ (2009) Response surface modeling of Pb (II) removal from aqueous solution by Pistacia vera L.: box–Behnken experimental design. J Hazard Mater 171:551–562
5. Ronteltap M, Maurer M, Gujer W (2007) The behaviour of pharmaceuticals and heavy metals during struvite precipitation in urine. Water Res 41:1859–1868
6. Mager EM, Brix KV, Gerdes RM, Ryan AC, Grosell M (2011) Effects of water chemistry on the chronic toxicity of lead to the cladoceran, Ceriodaphnia dubia. Ecotoxicol Environ Saf 74:238–243
7. Grover P, Rekhadevi PV, Danadevi K, Vuyyuri SB, Mahboob M, Rahman MF (2010) Genotoxicity evaluation in workers occupationally exposed to lead. Int J Hyg Environ Health 213:99–106
8. Murugesan GS, Sathishkumar M, Swaminathan K (2006) Arsenic removal from groundwater by pretreated waste tea fungal biomass. Bioresour Technol 97:483–487
9. Rao MM, Ramesh A, Rao GPC, Seshaiah K (2006) Removal of copper and cadmium from the aqueous solutions by activated carbon derived from Ceiba pentandra hulls. J Hazard Mater 129:123–129
10. Deng X, Lu L, Li H, Luo F (2010) The adsorption properties of Pb (II) and Cd (II) on functionalized graphene prepared by electrolysis method. J Hazard Mater 183:923–930
11. Nordberg GF, Flower BA, Nordberg M, Friberg L (2007) Handbook on the toxicology of metals academic press. The Netherlands, Amsterdam
12. Zhang X, Lin S, Lu XQ, Chen ZL (2010) Removal of Pb (II) from water using synthesized kaolin supported nanoscale zero-valent iron. Chem Eng J 163:243–248
13. Fu F, Wang Q (2011) Removal of heavy metal ions from wastewaters: a review. J Environ Manag 92:407–418
14. Singh CK, Sahu JN, Mahalik KK, Mohanty CR, Mohan BR, Meikap BC (2008) Studies on the removal of Pb (II) from wastewater by activated carbon developed from tamarind wood activated with sulphuric acid. J Hazard Mater 153:221–228
15. Park HG, Kim TW, Chae MY, Yoo IK (2007) Activated carbon-containing alginate adsorbent for the simultaneous removal of heavy metals and toxic organics. Process Biochem 42:1371–1377
16. Mohan D, Pittman Jr CU, Bricka M, Smith F, Yancey B, Mohammad J, Steele PH, Alexandre-Franco MF, Gomez-Serrano V, Gong H (2007) Sorption of arsenic, cadmium, and lead by chars produced from fast pyrolysis of wood and bark during bio-oil production. J Colloid Interface Sci 310:57–73
17. Dong L, Zhu Z, Qiu Y, Zhao J (2010) Removal of lead from aqueous solution by hydroxyapatite/magnetite composite adsorbent. Chem Eng J 165:827–834
18. Recillas S, García A, González E, Casals E, Puntes V, Sánchez A, Font X (2011) Use of CeO_2, TiO_2 and Fe_3O_4 nanoparticles for the removal of lead from water: toxicity of nanoparticles and derived compounds. Desalination 277:213–220
19. Samiey B, Cheng CH, Wu J (2014) Organic-inorganic hybrid polymers as adsorbents for removal of heavy metal ions from solutions: a review. Materials 7:673–726
20. Mercier L, Pinnavaia TJ (1998) Heavy metal ion adsorbents formed by the grafting of a thiol functionality to mesoporous silica molecular sieves: factors affecting hg (II) uptake. Environ Sci Technol 32:2749–2754
21. Kaşgöz H, Durmuş A, Kaşgöz A (2008) Enhanced swelling and adsorption properties of AAm-AMPSNa/clay hydrogel nanocomposites for heavy metal ion removal. Polym Adv Technol 19:213–220
22. Craciunescu I, Petran A, Liebscher J, Vekas L, Turcu R (2017) Synthesis and characterization of size-controlled magnetic clusters functionalized with polymer layer for wastewater depollution. Mater Chem Phys 185:91–97
23. Aiba M, Higashihara T, Ashizawa M, Otsuka H, Matsumoto H (2016) Triggered structural control of dynamic covalent aromatic polyamides: effects of thermal reorganization behavior in solution and solid states. Macromolecules 49:2153–2161
24. Banerjee S, Maji S (2011) Aromatic polyamides. High-performance processable aromatic polyamides. In: Mittal V (ed) High performance polymers and engineering plastics. Wiley, Hoboken, 111–166
25. Iwan A, Sek D (2008) Processible polyazomethines and polyketanils: from aerospace to light-emitting diodes and other advanced applications. Prog Polym Sci 33:289–345
26. Grigoras M, Catanescu O, Simionescu CI (2001) Poly (azomethine) s. Rev Roum Chim 46:927–939
27. Grigoras M, Catanescu CO (2004) Imine oligomers and polymers. J Macromol Sci C Polym Rev 44:131–173
28. Zhang LJ, Qi L, Chen XY, Liu F, Liu LJ, Ding WL, Li DL, Yuan GC, Tong JZ, Chen FY, Huang HJ (2018) Synthesis, crystal structure and photophysical properties of two reduced Schiff bases derived from 5-Aminoisophthalic acid. J Chem Crystallogr 1–7
29. Aghaei M, Kianfar AH, Dinari M (2019) Green synthesis of nanostructure Schiff base complex based on aromatic polyamide and manganese (III) for elimination of Hg (II) and Cd (II) from solutions. JICS 1–12
30. Rasool R, Hasnaina S, Nishata N (2014) Metal-based Schiff base polymers: preparation, spectral, thermal and their in vitro biological investigation. Des Monomers Polym 17:217–226
31. Lacroix PG, Di Bella S, Ledoux I (1996) Synthesis and second-order nonlinear optical properties of new copper (II), nickel (II), and zinc (II) Schiff-base complexes. Toward a role of inorganic chromophores for second harmonic generation. Chem Mater 8:541–545
32. Vitalini D, Mineo P, Di Bella S, Fragala I, Maravigna P, Scamporrino E (1996) Synthesis and matrix-assisted laser desorption ionization− time of flight characterization of an exactly alternating Copolycarbonate and two random Copolyethers containing Schiff Base copper (II) complex nonlinear optical units in the Main chain. Macromolecules 29:4478–4485
33. Kumar S, Jha RR, Yadav S, Gupta R (2015) Pd (II) complexes with amide-based macrocycles: syntheses, properties and applications in cross-coupling reactions. New J Chem 39:2042–2051
34. Tyagi M, Chandra S (2014) Synthesis and spectroscopic studies of biologically active tetraazamacrocyclic complexes of Mn (II), co (II), Ni (II), Pd (II) and Pt (II). J Saudi Chem Soc 18:53–58
35. Ebrahimipour SY, Mague JT, Akbari A, Takjoo R (2012) Synthesis, characterization, crystal structure and thermal behavior of 4-Bromo-2-(((5-chloro-2-hydroxyphenyl)imino)methyl phenol and its oxido-vanadium (V) complexes. J Mol Struct 1028:148–155
36. Kirupha SD, Murugesan A, Vidhyadevi T, Baskaralingam P, Sivanesan S, Ravikumar L (2012) Novel polymeric adsorbents bearing amide, pyridyl, azomethine and thiourea binding sites for the removal of Cu (II) and Pb (II) ions from aqueous solution. Sep Sci Technol 48:254–262
37. Dinari M, Haghighi A (2017) Efficient removal of hexavalent chromium and lead from aqueous solutions by s-triazine containing nanoporous polyamide. Polym Adv Technol 28:1683–1689
38. Dinari M, Mohammadnezhad G, Soltani R (2016) Fabrication of poly (methyl methacrylate)/silica KIT-6 nanocomposites via in situ polymerization approach and their application for removal of Cu^{2+} from aqueous solution. RSC Adv 6:11419–11429

39. Mohammadnezhad G, Dinari M, Soltani R (2016) The preparation of modified boehmite/PMMA nanocomposites by in situ polymerization and the assessment of their capability for Cu^{2+} ion removal. New J Chem 40:3612–3621
40. Zhengang L, Fu-Shen Z (2009) Removal of lead from water using biochars prepared from hydrothermal liquefaction of biomass. J Hazard Mater 167:933–939
41. Mishra PC, Patel RK (2009) Removal of lead and zinc ions from water by low cost adsorbents. J Hazard Mater 168:319–325
42. Kumari M, Pittman Jr CU, Mohan D (2014) Heavy metals [chromium (VI) and Lead (II)] removal from water using Mesoporous magnetite (Fe_3O_4) Nanospheres. J Colloid Interface Sci 442:120–132
43. El-Reash YA, Otto M, Kenawy IM, Ouf AM (2011) Adsorption of Cr (VI) and as (V) ions by modified magnetic chitosan chelating resin. Int J Biol Macromol 49:513–522
44. Langmuir I (1918) The adsorption of gases on plane surfaces of glass, mica and platinum. J Am Chem Soc 40:1361–1403
45. Naiya TK, Bhattacharya AK, Das SK (2008) Removal of Cd (II) from aqueous solutions using clarified sludge. J Colloid Interface Sci 325:48–56